Anisotropy in the compressive mechanical properties of bovine cortical bone and the mineral and protein constituents

Ekaterina Novitskaya [a,*], Po-Yu Chen [a], Steve Lee [a], Ana Castro-Ceseña [b], Gustavo Hirata [c], Vlado A. Lubarda [a,d], Joanna McKittrick [a,d]

[a] Materials Science and Engineering Program, University of California, San Diego, La Jolla, CA 92093, USA
[b] Centro de Investigación Científica y de Educación Superior de Ensenada, Ensenada, Mexico
[c] Centro de Nanociencias y Nanotecnologia, UNAM, Ensenada, Mexico
[d] Department of Mechanical and Aerospace Engineering, University of California, San Diego, La Jolla, CA 92093, USA

ARTICLE INFO

ABSTRACT

The mechanical properties of fully demineralized, fully deproteinized and untreated cortical bovine femur bone were investigated by compression testing in three anatomical directions (longitudinal, radial and transverse). The weighted sum of the stress–strain curves of the treated bones was far lower than that of the untreated bone, indicating a strong molecular and/or mechanical interaction between the collagen matrix and the mineral phase. Demineralization and deproteinization of the bone demonstrated that contiguous, stand-alone structures result, showing that bone can be considered an interpenetrating composite material. Structural features of the samples from all groups were studied by optical and scanning electron microscopy. Anisotropic mechanical properties were observed: the radial direction was found to be the strongest for untreated bone, while the longitudinal one was found to be the strongest for deproteinized and demineralized bones. A possible explanation for this phenomenon is the difference in bone microstructure in the radial and longitudinal directions.

© 2011 Acta Materialia Inc. Published by Elsevier Ltd. All rights reserved.

1. Introduction

Bone is a hierarchically structured composite material consisting mainly of a biopolymer (type I collagen), a mineral phase (carbonated hydroxyapatite) and water. There is also an amount of non-collagenous proteins that "glue" the collagen fibers together and attach the mineral to the collagen [1,2]. The structure and mechanical properties of the major bone constituents have been investigated by many research groups for several decades, including seminal works by Currey [3–5], Reilly and Burstein [6], Burstein et al. [7], and Rho et al. [8]. The mechanical properties of cortical bone are highly anisotropic, therefore, significant efforts have been made to examine the properties of bone in different anatomical directions [9–12]. Fig. 1 shows the orientation of the longitudinal, radial and transverse bone directions. One should keep in mind that measured strengths and stiffness values for bone are highly dependent on the test method, hydration condition, age, gender, histology, porosity and mineral content.

Reilly and Burstein [9] investigated the anisotropic compressive and tensile properties of cortical bone and found that the Young's modulus and maximum strength in the longitudinal direction are more than twice those in the transverse and radial directions. Bonfield and Grynpas [10] studied the mechanical anisotropy of cortical bone at varying angles to the bone growth direction (the longitudinal direction corresponded to 0°, the transverse direction to 90°) by ultrasonic measurement. They found that the Young's modulus gradually decreased with increasing angle (from 0° to 90°), and there was a plateau between 20° and 70°. Information on the mechanical properties in the radial direction was not reported. The bulk mechanical properties of bone are greatly affected by its microstructural features. Two types of bone are found in cortical bone, namely osteonal bone and periosteal bone, as shown in Fig. 1. Osteonal bone consists of osteons made up of thin (2–6 μm) lamellar sheets oriented in a concentric cylindrical structure. These osteons are 150–250 μm in diameter and align parallel along the long axis of bone. Interstitial lamellae (remnants after bone remodelling) occupy the space around the osteons. Periosteal bone consists of a circumferential lamellae structure which is parallel to the bone surface and is made of fibrolamellar bone. The periosteal bone is reported to be stronger and more highly anisotropic than osteonal bone [4]. The elastic properties of microstructural components in human and bovine osteonal bone have been investigated by several groups using nanoindentation. Rho et al. [13] showed that the Young's modulus of the interstitial lamellae (∼26 GPa) was higher than that in the osteons (∼22 GPa) in the longitudinal

* Corresponding author. Tel.: +1 858 534 55 13.
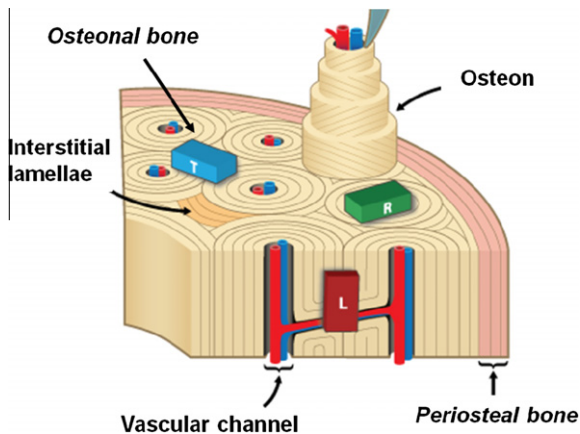E-mail address: eevdokim@ucsd.edu (E. Novitskaya).

Fig. 1. Schematic diagram of bone microstructure and sample orientations for the three anatomical directions in cortical bone. Sample orientations: L, longitudinal; R, radial; T, transverse. The samples are not shown to scale.

direction for human cortical bone. The average Young's modulus (including both osteons and interstitial lamellae) in the transverse direction was found to be ~17 GPa. Swadener et al. [14] and Fan et al. [15] proposed and verified methods to predict the nanoindentation moduli for different bone directions based on the previous ultrasound studies by Rho [16]. A possible mechanism for bone anisotropy at the 10–100 μm scale was suggested by Seto et al. [17]. They performed tensile experiments on relatively small samples (a fibrolamellar unit) obtained from the periosteal region (see Fig. 1). An extremely high mechanical anisotropy in the Young's modulus (of the order of 1:20) and tensile strength (of the order of 1:15) between the transverse and longitudinal directions in wet bovine femur bone was reported. Furthermore, they proposed that the periodic presence of mechanically weak heterogeneous layers filled with soft organic constituents inside the fibrolamellar bone accounted for this high anisotropy. These weak interfaces act as damping elements and suppress crack propagation on the 10–100 μm scale.

One of the main reasons for bone anisotropy is the preferential orientation of collagen fibers and mineral crystals along the bone growth direction. This topic has been investigated by several groups [18–20]. Landis et al. [18] investigated the ultrasound interaction between collagen and mineral crystals in chicken bone by high voltage electron microscopic tomography and found that individual platelet-shaped mineral crystals were periodically arranged along collagen fibrils preferentially aligned along the main bone axis. Martin et al. [19,20] found that the longitudinal fiber orientation in cortical bone contributed greatly to the increased elastic modulus and strength in four point bending.

The mineral/protein interaction is important to understand how bone constituents affect the mechanical properties. The mechanical properties of the protein and mineral constituents can be investigated separately by demineralization and deproteinization, respectively. Mechanical testing results in compression and tension on deproteinized bone were summarized by Piekarski [21] and Mack [22], but information on the orientation of the bone was not provided. Burstein et al. [7] investigated the tensile mechanical properties of partially demineralized bone using HCl solution at varying concentration. They found that bone in tension demonstrated plastic behavior: the yield point and maximum strength progressively decreased as demineralization proceeded, while the slope of the plastic region was the same for all demineralization stages. These findings demonstrated that bone stiffness in the plastic region is a function of collagen properties only. The

contribution of the two main bone constituents to elastic anisotropy was investigated by Hasegawa et al. [11] and Iyo et al. [23]. Hasegawa et al. [11] performed acoustic velocity measurements on demineralized and deproteinized dog femur in the longitudinal and transverse directions. They found that the collagen matrix is highly isotropic and proposed that the minerals play the major role in the anisotropic behavior of whole bone. Iyo et al. [23] investigated the effect of mechanical anisotropy on Young's modulus relaxation. Their model consisted of a combination of two processes: a fast one, attributed to relaxation of the collagen matrix, and a slow one, attributed to the mixture of collagen and mineral phases. Moreover, they suggested that the latter process, corresponding to both collagen and mineral constituents, was responsible for the anisotropic behavior of bone, in contrast to what had been suggested by Hasegawa et al. [11]. A detailed examination of the mechanical properties of the major bone constituents (mineral and collagen parts) in different anatomical directions is important to better understand the mechanical behavior of bone. Skedros et al. [24] used acoustic microscopy to evaluate the elastic modulus of untreated, demineralized and deproteinized cortical bone of deer calcanei for different bone cortices. It was found that the anisotropy ratio, defined as the ratio between the acoustic velocity squared for the longitudinal and transverse bone directions, was significantly different from that for both demineralized and deproteinized bone, demonstrating that not only untreated bone, but also the main bone constituents (the mineral and collagen phases) were anisotropic. The anisotropy ratio was higher for cortices that were adapted for tension and compression, and were less for cortices that were adapted for a combination of compression/shear or tension/shear. These results clearly indicate that the degree of anisotropy of bone greatly depends on its functions and adaptations. Macione et al. [12] investigated the properties of partially demineralized bone using an ultrasound technique. They showed that the elastic modulus in the longitudinal direction could be predicted using ultrasound measurements on the transverse and radial directions.

The mechanical properties of demineralized and deproteinized cancellous bone were recently studied by several groups. Chen et al. [25] developed and verified methods to fully demineralize and fully deproteinize cancellous bovine femur bone without altering the microstructure. It was found that minerals form a continuous, stand-alone structure after removing all the protein, and mature cancellous bone was indeed an interpenetrating composite, in agreement with Rosen et al. [26], who found a well-organized mineral structure in deproteinized bovine cortical bone. The compressive mechanical properties of demineralized and deproteinized cancellous bone were further investigated by Chen and McKittrick [27]. It was shown that both the relative elastic modulus and compressive strength increased with relative density. Moreover, a strong synergistic effect between the mineral and protein phases was found and rule of mixture did not apply, proving strong chemical bonding and interactions between the two phases. Lubarda et al. [28] derived the elastic modulus of untreated cancellous bone based on the measured properties of the mineral and protein phases in order to understand osteoporotic degradation. The demineralization kinetics for cancellous and cortical bone were thoroughly studied by Castro-Ceseña et al. [29]. It was shown that the mineral and protein phases of cortical bone are independent structures that can be mechanically tested, corroborated the findings of Chen et al. [25], but mechanical testing was not performed.

To the best of our knowledge there has been no study of the mechanical properties of demineralized and deproteinized cortical bone as a function of anatomical direction, which is the goal of this study.

2. Materials and methods

2.1. Sample preparation

Bovine femur bone samples were obtained from a local butcher. The slaughter age of cattle was about 18 months. The bone was thoroughly cleaned with water. About 100 samples for compression testing (parallelepipeds $5 \times 5 \times 7.5$ mm) were prepared from adjacent areas of the bone in order to minimize variations in density and mineral content. The samples were first roughly cut with a handsaw and then with a diamond blade with the surfaces cut as parallel as possible. Samples were cut in all three anatomical directions (Fig. 1). The longitudinal direction was chosen to be parallel to the growth direction of the bone, the transverse direction was normal to the bone growth direction, and the radial one was orthogonal to both. Samples were stored in a refrigerator until the chemical procedures and testing were performed.

2.2. Demineralization and deproteinization

Bone samples were demineralized (DM) by aging in 0.6 N hydrochloric acid (HCl) at room temperature using the procedures outlined in Toroian et al. [30] and Chen et al. [25]. It should be noted that although EDTA (ethylenediaminetetraacetic acid) has been used to demineralize bone [31], complete demineralization may require 1 month or more at 37 °C, which thus may damage the gross structure of the matrix (possibly due to enzymatic autolysis). Consequently, we chose HCl as the demineralization medium, since the process is much quicker at room temperature, minimizing damage to the protein structure. Acid solutions were changed every 2 h in order to avoid saturation, which can affect the demineralization rate process. The whole process took about 50 h. The completeness of demineralization was verified by mineral absence in the solution using the procedure described in Castro-Ceseña et al. [29]. Bone samples were deproteinized (DP) by aging in a 5.6 wt.% sodium hypochlorite (NaOCl) solution at 37 °C, following the procedure outlined in Chen et al. [25]. The solutions were changed every 6 h. The whole process took about 2 weeks.

2.3. Compression testing

Three different sets of the samples were prepared: 40 untreated (UT), 30 demineralized (DM) and 30 deproteinized (DP). Specimens from all groups were submerged in Hank's balanced saline solution for 24 h before testing, and were tested in the hydrated condition. Compression testing of UT bone samples was performed in a universal testing machine equipped with a 30 kN load cell (3367 Dual Column Testing System, Instron, Norwood, MA). Compression testing of DM and DP bone samples was performed in a universal testing machine equipped with a 500 N load cell (3342 Single Column System, Instron, Norwood, MA). Compression testing for samples from all three groups was performed at a strain rate of 1×10^{-3} s^{-1}. An external deflectometer SATEC model I3540 (Epsilon Technology Corp., Jackson, WY) was used in order to measure the small displacements. All samples were loaded until compressive failure. Compressive failure is defined in the following sections for UT, DM and DP samples.

2.4. Structural characterization

Samples from the all groups were analyzed by optical microscopy using a Zeiss Axio imager equipped with a CCD camera (Zeiss Microimaging Inc., Thornwood, NY). Fracture surfaces of the specimens were investigated by scanning electron microscopy (SEM)

equipped for energy-dispersive spectroscopy (EDS) (FEI-XL30, FEI Company, Hillsboro, OR). DM samples were subjected to critical point drying before SEM imaging in order to avoid excessive shrinkage. For SEM imaging all samples were mounted on aluminum sample holders, air dried and sputter coated with chromium before imaging. Samples were observed at a 20 keV accelerating voltage.

2.5. Statistical analysis

Since the UT and DP bone samples fail in a brittle manner, as they contain pre-existing flaw size distributions [32], the compressive strengths were analyzed by the Weibull probability distribution, which is a powerful method to analyze statistical variations in the strength of materials. The Weibull distribution function [33] provides the failure probability (F), which depends on the failure stress (σ_f), according to:

$$F(\sigma_f) = 1 - \exp\left(\frac{\sigma_f}{\sigma_0}\right)^m \tag{1}$$

where σ_0 is the characteristic strength of the material (stress at which 63.2% of the samples have failed, when $\sigma_f = \sigma_0$), and m is the Weibull modulus. A larger value of m indicates less variability in the strength distribution. The average compressive strength ($\bar{\sigma}$) was taken as the mean of the Weibull distribution, according to [34]:

$$\bar{\sigma} = \sigma_0 \Gamma\left(1 + \frac{1}{m}\right) \tag{2}$$

$$\Gamma\left(1 + \frac{1}{m}\right) = \int_0^\infty x^{1/m} e^{-x} dx \tag{3}$$

where Γ is the Gamma function, defined by the indicated improper integral, whose values are tabulated in Abramowitz and Stegun [35].

3. Results and discussion

Fig. 2 shows photographs of UT, DM and DP cortical bovine femur bone. Demineralization and deproteinization of cortical bone produced contiguous, stand-alone structures that can be tested for their mechanical properties. Moreover, Fig. 2 demonstrates that cortical bone can be considered a "two phase" interpenetrating composite material, which according to Mack [22] achieves superb mechanical properties by interaction between the mineral and protein phases, which make the properties of bone superior to the properties of its individual (mineral and protein) components as separate phases, corroborating the findings of Chen et al. [25], who reported the same for bovine femur cancellous bone. Fig. 3 shows SEM images of fracture surfaces for UT, DM and DP bone.
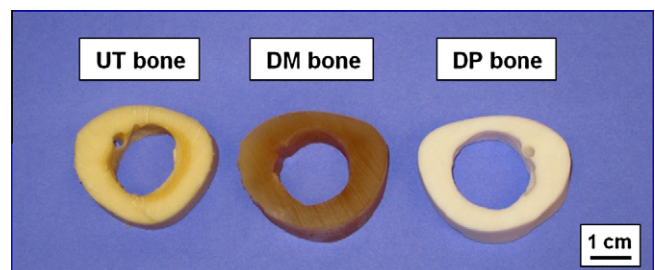

Fig. 2. Photographs of untreated (UT), fully demineralized (DM) and fully deproteinized (DP) cortical bovine femur bone. The DM and DP samples are continuous, stand-alone structures that can be tested for mechanical properties (courtesy of Professor Paul Price, UCSD).
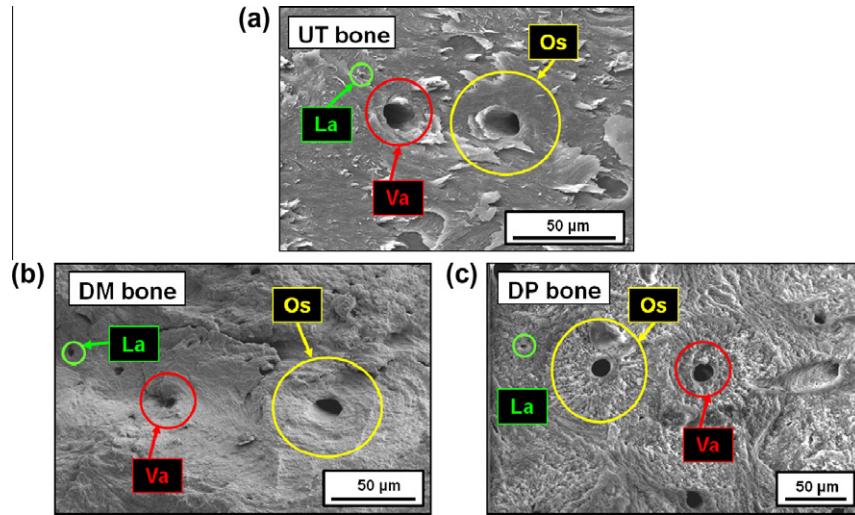
Fig. 3. SEM images of (a) untreated (UT), (b) demineralized (DM) and (c) deproteinized (DP) bovine cortical bone (fracture surfaces). Os, osteons; La, lacuna spaces; Va, vascular channels. Images were taken from different samples.
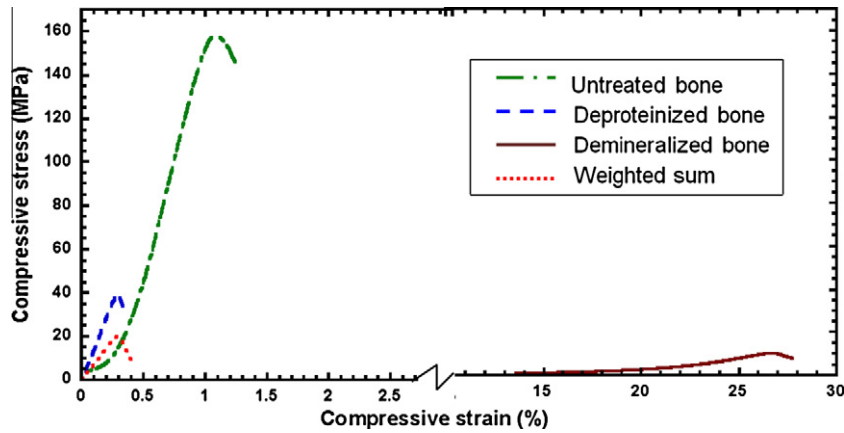

Fig. 4. Average stress–strain curves for untreated, deproteinized and demineralized cortical bovine femur bone tested in the longitudinal direction. The calculated weighted sum (dots) clearly underestimates the properties of untreated bone.

The images were taken from the different samples. SEM images of the DM (Fig. 3b) and DP samples (Fig. 3c) showed that the collagen fibers in the former case and minerals in the latter case are aligned in a coherent manner, forming a continuous network. Moreover, microscopic features, such as vascular channels (10–20 μm in diameter) and lacunae (5–10 μm in diameter) are preserved in both the DP and DM samples, in agreement with Chen et al. [25]. Well-defined osteonal structures are clearly observed in both the DP and DM images, as well as in the UT image (Fig. 3a).

Stress–strain curves for UT, DM and DP bone in the longitudinal direction are shown in Fig. 4. The weighted sum of the stress–strain curves (σ_s) for the DM and DP samples is shown, which, based on the Voigt averaging scheme, is:

$$\sigma_s = f_m \sigma_m + f_p \sigma_p = f_m \sigma_m + (1 - f_m)\sigma_p \qquad (4)$$

where f_m is the volume fraction of the mineral phase and σ_m and σ_p are the stresses in the mineral and protein phases, respectively. Using $f_m \approx 0.5$ the Voigt average curve is far lower than that of UT bone (Fig. 4). This indicates a strong molecular interaction or mechanical interlocking between the proteins and minerals. More involved models for determining the effective elastic properties of heterogeneous materials, or materials weakened by voids of

different size and geometry, such as the self-consistent method or the differential scheme [36], could be utilized to account for some of the interactions that take place at higher concentration of collagen as the weaker phase, but these models are beyond the scope of this work. The UT and DP samples fractured in a brittle manner (Figs. 4 and 5a and c), while the DM samples showed behavior typical for collagen, with a long toe region at small strains (Figs. 4 and 5b).

Fig. 5a–c shows the compression stress–strain curves for UT, DM and DP bone samples in the three anatomical directions, clearly exhibiting the highly anisotropic properties. The compressive strength was identified at fracture point for the UT and DP samples, and as the maximum compressive stress for the DM samples. The longitudinal direction is the strongest and stiffest for DP and DM bone, while the radial one is the strongest for UT bone. The porosity of DM and DP bone is much higher than that of UT bone, due to the treatment generated pores, dominantly extended in the longitudinal direction. This yields a lower stiffness in the radial and transverse directions compare to the longitudinal direction. Additionally, the radial direction is the toughest (area under stress–strain curve) direction for UT bone. The collagen and mineral phases both play a significant role in bone mechanical properties, therefore UT bone has superior properties to either the mineral
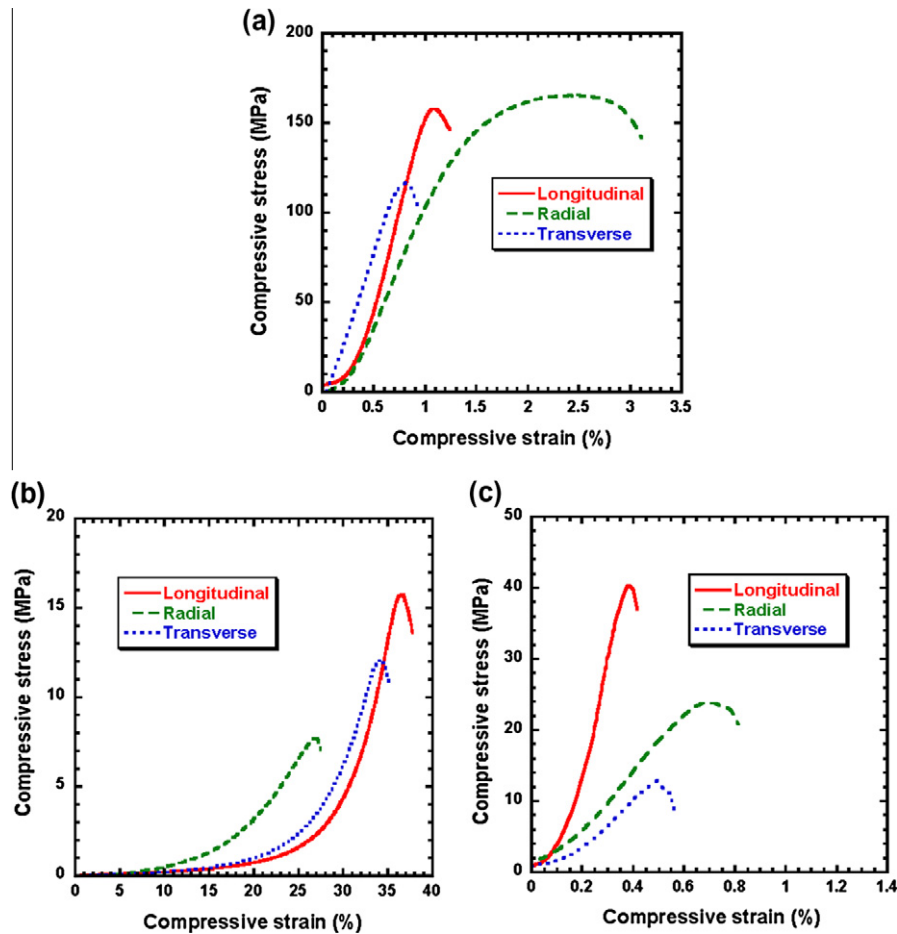
Fig. 5. Representative compression stress–strain curves for the three anatomical directions for (a) untreated, (b) demineralized and (c) deproteinized bone.

or collagen parts. Therefore, when either phase is removed the bonds between the collagen and mineral phases are broken, which significantly affects the mechanical properties. Minerals preferentially orient in the longitudinal direction [1,18], therefore this direction is the strongest and stiffest direction for DP bone. Furthermore, collagen fibers are also preferentially oriented in the longitudinal direction [1,19,20], therefore the longitudinal direction is also the stiffest and strongest direction for DM bone. These findings support the idea of Iyo et al. [23] and Skedros et al. [24] that both the mineral and the collagen constituents contribute to the anisotropic behavior of cortical bone. We have shown that not only UT bone is anisotropic, but also DM and DP bone (see Table 1 and

Fig. 5). Weibull distributions for the compressive strengths of UT and DP bone (Fig. 6) clearly demonstrate that the radial direction is strongest for UT bone, while the longitudinal one is strongest for DP bone. A somewhat less perfect fit of the Weibull plot to the experimental data for UT bone in the radial direction is a consequence of a less uniform microstructure of the samples used for testing in the radial direction (see Fig. 7a for the transverse direction and Fig. 7b for the radial direction).

Table 1 summarizes the hydrated density, average compressive strength, Young's modulus, and Weibull modulus for UT, DP and DM bone in the three anatomical directions. The Weibull moduli are listed only for the UT and DP samples, as the DM samples did

Table 1
Hydrated density, Young's modulus, compressive strength and compressive strength Weibull modulus (m) for untreated (UT), deproteinized (DP) and demineralized (DM) bovine cortical bone in the three anatomical directions.

Sample	Orientation	Density (g cm^{-3})	Young's modulus (GPa)	Average compressive strength (MPa)	m
UT	L	2.06 ± 0.01	22.6 ± 1.2	120 ± 9	3.32
	R	2.03 ± 0.05	12.4 ± 0.4	142 ± 13	4.22
	T	2.04 ± 0.04	16.2 ± 1.4	112 ± 7	5.68
DP	L	2.00 ± 0.01	9.2 ± 2.8	24 ± 4	2.04
	R	1.94 ± 0.01	2.6 ± 0.5	18 ± 3	2.32
	T	1.96 ± 0.01	2.2 ± 0.3	11 ± 1	2.95
DM	L	1.17 ± 0.01	0.232 ± 0.009	14 ± 1	N/A
	R	1.17 ± 0.01	0.060 ± 0.009	6 ± 1	N/A
	T	1.18 ± 0.01	0.132 ± 0.015	11 ± 1	N/A

The Weibull moduli (m) are listed for the UT and DP bone samples. The DM samples did not fracture. L, longitudinal; R, radial; T, transverse (Fig. 1). The average compressive strength was taken as the mean Weibull distribution according to Eq. (2) for UT and DP bone. For DM bone the compressive strength was taken as the maximum stress from the stress–strain curves. The Young's modulus was estimated from the steepest portion of the stress–strain curves for all samples.
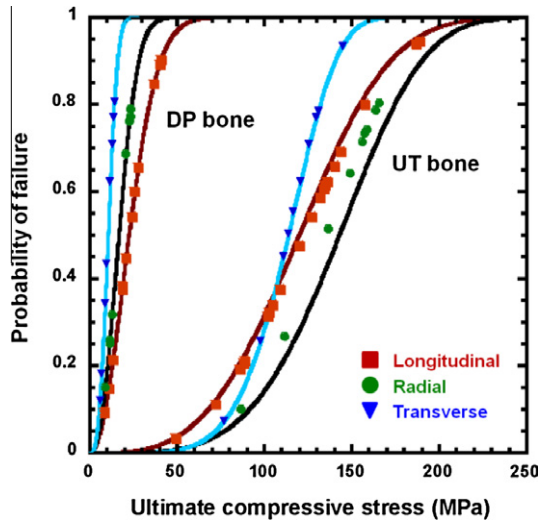
Fig. 6. Weibull plots for ultimate compressive stress for untreated (n(L) = 20; n(R) = 10; n(T) = 10), and deproteinized (n(L) = 12; n(R) = 10; n(T) = 10) bone. Demineralized bone is 100% protein and Weibull analysis was therefore not applicable.

not break in a brittle manner. The average compressive strength was calculated according to Eq. (2) for UT and DP bone, and as the mean compressive strength for DM bone. The first observation is the density values: the densities of the DM samples are much smaller than those of the DP samples because the density of pure collagen (1.35 g cm^{-3}) [37] is almost three times less than the density of pure hydroxyapatite (3.15 g cm^{-3}) [38]. These findings are well correlated with Chen et al. [25]. Another interesting observation was that the hydrated DP density values are very close to the UT ones, which indicates that water fills all or nearly all of the empty voids created after protein removal (since the density of water (1 g cm^{-3}) is slightly less than that of collagen, and that of the hydrated DP sample density is slightly less than that of UT ones).

Next, for the UT bone there are clear differences in the stiffness values in the longitudinal, transverse and radial directions. The longitudinal and transverse stiffness values correlate well with that of human femur [39], and show that the longitudinal stiffness is 30% higher than the transverse stiffness. This can be attributed to several factors. First, the collagen is aligned in the longitudinal direction, with the coexisting mineral orientation in the same direction. Applying the Voigt and Reuss models of aligned fibrous composites, the stiffness in the longitudinal direction is predicted to be about 22 times higher than in the transverse direction. Another factor is the osteon structure, which is aligned in the longitudinal direction. The interior vascular channels are hollow cylinders that, when compressed in the transverse direction, will deform more easily than in the longitudinal direction.

In addition, the average longitudinal Young's modulus for the UT, DP and DM bone samples were 22.6, 9.2 and 0.232 GPa, respectively. These results indicate that the majority of the stiffness comes from the mineral contribution, as expected. The elastic modulus of DP bone was almost three times lower compared with UT bone, because of the significantly increased porosity (from 10 to 55 vol.%) induced by the deproteinization process. The average Young's moduli for UT, DP and DM radial and transverse samples show a similar trend, but with smaller differences in the Young's modulus values between the UT and DP cases. In addition, the average Young's modulus drops about 100 times between the UT and DM samples for all three anatomical directions, proving that the majority of the bone stiffness comes from the mineral phase, and the collagen phase makes only a small contribution to the overall bone stiffness.

Furthermore, it is clear that the weighted sum of the compressive strength for the pure mineral (DP samples) and pure protein phases (DM samples) is not even close to the compressive strength of the UT samples for all three anatomical directions (Fig. 4). These findings clearly support the conclusion that bone mechanical properties should be evaluated as properties of an interpenetrating composite rather than being a simple sum of the properties of its two main components properties.

The Weibull modulus appears to be highest for the transverse direction for both UT and DP bone. This means that bone behaves in the most predictive way in this particular direction (strength is most equally distributed in the bone volume for this direction). Strength in the longitudinal direction, in contrast, appears to be the most scattered for both cases. It can be attributed to longitudinal alignment of the collagen fibers and minerals, as well as the presence of vascular channels.
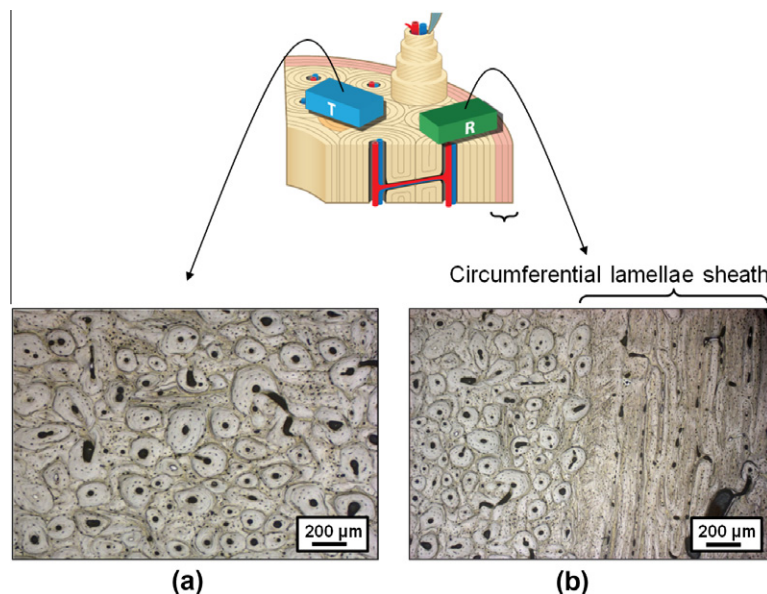

Fig. 7. Optical micrographs showing the structure differences between (a) transverse, and (b) radial bone samples. Circumferential lamellae sheath is clearly shown at (b).

The difference in mechanical behavior between the radial and transverse directions for UT bone (Table 1 and Fig. 5a) is unexpected – they should be similar, as the osteons are perpendicular to the loading direction in both cases. The cortical bone microstructure is shown in Fig. 7. The outer part of the bone near the bone surface (the periosteal part) consists of a circumferential lamellae structure that is parallel to the bone surface [40]. This region has a thickness of ~600 μm, consisting of 15–20 lamellae. In addition, the mineralized collagen fibers in each of the lamella are oriented at different angles, giving the bone extra strength in the radial direction. Optical micrographs of radial and transverse samples (cross-sectional view) are shown in Fig. 7. The outer part of the bone of radial sample consists of a thin layer (Fig. 7b) that is organized differently to the rest of the bone volume (Fig. 7a). Moreover, mineralized collagen lamellae in this thin outer layer are not developed cylindrical osteons, but are arranged smoothly in the longitudinal direction (Fig. 7b), creating an outer sheath. This sheath contributed to the mechanical response of samples taken in the radial direction, as the bone is too narrow in this direction to cut samples that do not contain this sheath, but it does not contribute to the properties of transverse samples (Figs. 1 and 7a). Therefore, the differences in mechanical properties between the radial and transverse directions for UT bone were attributed to the existence of the radial sheath (periosteal bone with a different microstructure). For the same reason the UT bone samples were found to be stronger in the radial than in the longitudinal direction.

The fact that the longitudinal direction appears to be the strongest direction for DP bone can be explained by consideration of the stress concentration factor. Compression of DP bone can be considered as compression of a solid with a pre-existing micro flaw size distribution due to the high porosity (~55%). During the DP process the voids (considered as interconnected ellipses in our 2D model sketched in Fig. 8) appear at those places previously occupied by the protein matrix. Since collagen fibers are preferentially aligned in the bone growth direction (longitudinally), the voids are preferentially oriented in this direction. This additional porosity level for the longitudinal and transverse (or radial) directions is shown in Fig. 8, which shows that the elliptical major axis is parallel to the loading direction for the longitudinal orientation and is perpendicular for the transverse and radial orientations. Ignoring the void interactions effects [36], the stress concentration factor (K) for points A and B is about the same for the longitudinal direction,

but greatly differ from each other for the transverse and radial directions, and is given by:

$$K_A = \sigma_a \left(1 + 2\frac{a}{b}\right) \tag{5}$$

$$K_B = \sigma_a \tag{6}$$

where σ_a is the applied stress, a and b are the lengths of the major and minor axes, respectively, of the elliptically shaped void. As long as the collagen phase is a continuous bone phase, there are some voids of smaller size and concentration that appear at places of interconnectivity of collagen fibers, preferentially oriented in the longitudinal direction. This additional porosity weakens DP bone in both the longitudinal and radial/transverse directions, but the weakening effect is less pronounced in the longitudinal direction, which results in superior properties of DP bone in that direction, as predicted by Eqs. (5) and (6). Consequently, the longitudinal direction is the stiffest and strongest direction for DP bone, supporting the findings shown in Figs. 5c and 6.

4. Conclusions

The mechanical properties and microstructure of untreated (UT), demineralized (DM) and deproteinized (DP) cortical bone for three anatomical directions were investigated. The main findings are as follows.

- UT, DM and DP cortical bovine femur bone all show anisotropic mechanical behavior.
  - The radial direction is the strongest for UT bone due to existence of a thin layer of circumferential lamellae (periosteal bone) that provides extra strength in this direction.
  - The longitudinal direction is the stiffest and strongest for DM and DP bone due to the preferential orientation of either the collagen fibers (DM bone) or minerals (DP bone) in the longitudinal direction.
- The weighted sum of the DP and DM strengths for all three anatomical directions is not equal to the strength of the UT bone, proving a strong interaction between the two main bone constituents.
- The Young's modulus decreases almost 100 times between the UT and DM bone samples, indicating that the greater part of the bone stiffness comes from the mineral contribution.
- The difference in Young's modulus between the longitudinal and transverse/radial directions for DP bone could be explained by the existence of elliptically shaped porosities oriented along the major axis parallel to the bone growth direction, resulting in different stress concentrations for the different directions.

Appendix A. Figures with essential colour discrimination

Certain figures in this article, particularly Figures 1–8, are difficult to interpret in black and white. The full colour images can be found in the on-line version, at doi: 10.1016/j.actbio.2011.04.025.
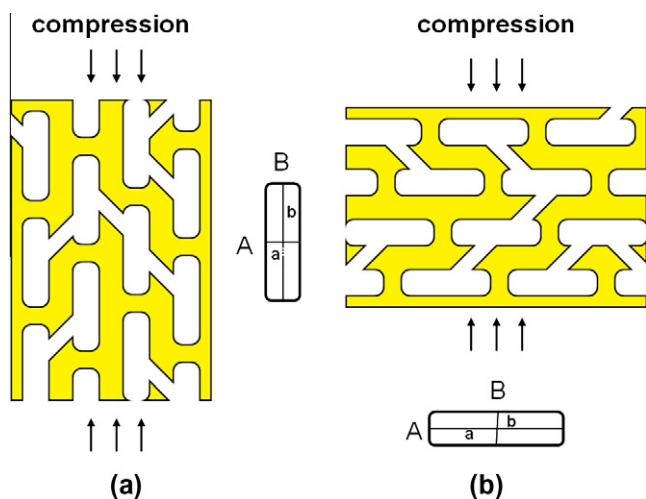

Fig. 8. Illustration of the preferentially oriented porosity level after collagen matrix removal for: (a) longitudinal, and (b) transverse/radial directions under compression for deproteinized cortical bone.

References

[1] Olszta MJ et al. Bone structure and formation: a new perspective. Mater Sci Eng R 2007;58:77–116.

[2] Thurner PJ, Lam S, Weaver JC, Morse DE, Hansma PK. Localization of phosphorylated serine, osteopontin, and bone sialoprotein on bone fracture surfaces. J Adhes 2009;85:526–45.

[3] Currey JD. The mechanical properties of bone. Clin Orthop Relat Res 1970;73:210–31.

[4] Currey JD. Bones: structure and mechanics. New York: Princeton University Press; 2002. p. 12–21.

[5] Currey JD. Measurement of the mechanical properties of bone: a recent history. Clin Orthop Relat Res 2009;467:1948–54.

[6] Reilly DT, Burstein AH. The mechanical properties of cortical bone. J Bone Joint Surg Am 1974;56:1001–22.

[7] Burstein AH, Zika JM, Heiple KG, Klein L. Contribution of collagen and mineral to the elastic-plastic properties of bone. J Bone Joint Surg Am 1975;57:956–61.

[8] Rho JY, Kuhn-Spearing L, Zioupos P. Mechanical properties and the hierachical structure of the bone. Med Eng Phys 1998;20:92–102.

[9] Reilly DT, Burstein AH. The elastic and ultimate properties of compact bone tissue. J Biomech 1975;8:393–405.

[10] Bonfield W, Grynpas MD. Anisotropy of the Young's modulus of bone. Nature 1977;270:453–4.

[11] Hasegawa K, Turner CH, Burr DB. Contribution of collagen and mineral to the elastic anisotropy of bone. Calcif Tissue Int 1994;55:381–6.

[12] Macione J, DePaula CA, Guzelsu N, Kotha SP. Correlation between longitudinal, circumferential, and radial moduli in cortical bone: effect of mineral content. J Mech Behav Biol Mater 2010;3:405–13.

[13] Rho JY, Roy II ME, Tsui TY, Pharr GM. Elastic properties of microstructural components of human bone tissue as measured by nanoindentation. J Biomed Mater Res 1999;45:48–54.

[14] Swadener JG, Rho JY, Pharr GM. Effects of anisotropy on elastic moduli measured by nanoindentation in human tibial cortical bone. J Biomed Mater Res 2001;57:108–12.

[15] Fan Z, Swadener JG, Rho JY, Roy ME, Pharr GM. Anisotropic properties of human tibial cortical bone as measured by nanoindentation. J Ortho Res 2002;20:806–10.

[16] Rho JY. An ultrasonic method for measuring the elastic properties of human tibial cortical and cancellous bone. Ultrasonics 1996;34:777–83.

[17] Seto J, Gupta HS, Zaslansky P, Wagner HD, Fratzl P. Tough lessons from bone: extreme mechanical anisotropy at mesoscale. Adv Funct Mater 2008;18:1905–11.

[18] Landis WJ, Hodgens KJ, Arena J, Song MJ, McEwen BF. Structural relations between collagen and mineral in bone as determined by high voltage electron microscopic tomography. Microsc Res Tech 1996;33:192–202.

[19] Martin RB, Boardman DL. The effects of collagen fiber orientation, porosity, density, and mineralization of bovine cortical bone bending properties. J Biomech 1993;26:1047–54.

[20] Martin RB, Lau ST, Mathews PV, Gibson VA, Stovert SM. Collagen fiber organization is related to mechanical properties and remodeling in equine bone. A comparison of two methods. J Biomech 1996;29:1515–21.

[21] Piekarski K. Analysis of bone as a composite material. Int J Eng Sci 1973;11:557–65.

[22] Mack RW. Bone – a natural two-phase material. Tech Mem Biomech Lab. Berkeley: University of California; 1964.

[23] Iyo T, Maki Y, Sasaki N, Nakata M. Anisotropic viscoelastic properties of cortical bone. J Biomech 2004;37:1433–7.

[24] Skedros JG, Sorenson SM, Takano Y, Turner CH. Dissociation of mineral and collagen orientations may differentially adapt compact bone for regional loading environments: results from acoustic velocity measurements in deer calcanei. Bone 2006;39:143–51.

[25] Chen P-Y, Toroian D, Price PA, McKittrick J. Minerals form a continuum phase in mature cancellous bone. Calc Tiss Int 2011;88:351–61.

[26] Rosen VB, Hobbs LW, Spector M. The ultrastructure of anorganic bovine bone and selected synthetic hydroxyapatites used as bone graft substitute materials. Biomaterials 2002;23:921–8.

[27] Chen P-Y, McKittrick J. Compressive mechanical properties of demineralized and deproteinated cancellous bone. J Mech Behav Biol Mater, in press, <doi:10.1016/j.jmbbm.2011.02.006>.

[28] Lubarda VA, Novitskaya EE, Bodde SG, McKittrick J, Chen PY. Elastic properties of cancellous bone in terms of elastic properties of its mineral and protein phase with application to their osteoporotic degradation, Mech Mater, accepted for publication.

[29] Castro-Ceseña AB, Novitskaya EE, Chen P-Y, Hirata GA, McKittrick J. Kinetic studies of bone demineralization at different HCl concentrations and temperatures. Mater Sci Eng C 2011;31:523–30.

[30] Toroian D, Lim JL, Price PA. The size exclusion characteristics of type-I collagen: implications for the role of non-collagenous bone constituents in mineralization. J Biol Chem 2007;282:22284–437.

[31] Broz JJ, Simske SJ, Greenberg AR. Material and compositional properties of selectively demineralized cortical bone. J. Biomech 1995;28:1357–68.

[32] Meyers MA, Chawla KC. Mechanical behavior of materials. New York: Cambridge University Press; 2009. p. 449–457.

[33] Weibull W. A statistical distribution function of wide applicability. J Appl Mech 1951;18:293–7.

[34] Rinne H. The Weibull distribution: a handbook. Boca Raton, FL: Chapman & Hall/CRC Press; 2008.

[35] Abramowitz M, Stegun IA. Handbook of mathematical functions with formulas, graphs, and mathematical tables. New York: Dover Publications; 1972.

[36] Gross D, Seeling T. Micromechanics and homogenization. Fracture mechanics with an introduction to micromechanics. New York: Springer; 2006. p. 218–87.

[37] Heidermann E, Riess W. Die Veranderungen Des Kollagens Bei Entwasserung Mit Aceton + Die Konsequenzen Dieser Veranderung Fur Die Kollagenstruktur. Hoppe-Seyler's Z Physiol Chem 1964;337:101.

[38] Potoczek M. Hydroxyapatite foams produced by gelcasting using agarose. Mater Lett 2008;62:1055–7.

[39] Wainwright SA, Biggs WD, Currey JD, Gosline JM. Mechanical design in organisms. New York: Wiley; 1976. p. 174–81.

[40] Fung YC. The anatomy of a long bone. Biomechanics: mechanical properties of living tissues. New York: Springer-Verlag; 1981. p. 384–9.